The Journal of Experimental Biology 210, 2033-2045
Published by The Company of Biologists 2007
doi:10.1242/jeb.000976

# Physiological and morphological responses to feeding in broad-nosed caiman (*Caiman latirostris*)

J. Matthias Starck[1,*], Ariovaldo P. Cruz-Neto[2] and Augusto Shinya Abe[2,3]

[1]*Department of Biology, University of Munich (LMU), Munich, Germany,* [2]*Department of Zoology, State University of São Paulo, Rio Claro, Brazil and* [3]*CAUNESP, State University of São Paulo, Rio Claro, Brazil*

*Author for correspondence (e-mail: starck@uni-muenchen.de)

*Accepted 7 March 2007*

## Summary

**Broad nosed caiman are ectotherm sauropsids that naturally experience long fasting intervals. We have studied the postprandial responses by measuring oxygen consumption using respirometry, the size changes of the duodenum, the distal small intestine, and the liver, using repeated non-invasive ultrasonography, and by investigating structural changes on the level of tissues and cells by using light- and electron microscopy. The caimans showed the same rapid and reversible changes of organ size and identical histological features, down to the ultrastructure level, as previously described for other ectothermic sauropsids. We found a configuration change of the mucosa epithelium from pseudostratified during fasting to single layered during digestion, in association with hypertrophy of enterocytes by loading them with lipid droplets. Similar patterns were also found for the hepatocytes of the liver. By placing the results of our study in comparative relationship and by utilizing the phylogenetic bracket of crocodiles, birds and squamates, we suggest that the observed features are plesiomorphic characters of sauropsids. By extending the comparison to anurans, we suggest that morphological and physiological adjustments to feeding and fasting described here may have been a character of early tetrapods. In conclusion, we suggest that the ability to tolerate long fasting intervals and then swallow a single large meal as described for many sit-an-wait foraging sauropsids is a functional feature that was already present in ancestral tetrapods.**

Key words: specific dynamic action, postprandial, metabolism, gastrointestinal tract, crocodiles, ultrasonography.

## Introduction

Seasonal pattern of food availability determine periods of feeding and fasting in many carnivorous and herbivorous sauropsids. Broad nosed caimans, *Caiman latirostris*, inhabit shallow marshes and ephemeral ponds in tropical and subtropical South America (Scott et al., 1990). They naturally experience fasting periods of several months because of seasonal fluctuations of food availability (Gorzula, 1978). During the rainy season (January to May), they find plenty of food (fish, crabs, snails, terrestrial vertebrates) in rivers and ponds. During the dry season (June to December), the caimans bury themselves in the bottom mud (Dixon and Soini, 1977) or retreat into relatively small ponds where they crowd together reaching high densities (Schaller and Crawshaw, 1982). Then, prey disappears quickly from those ponds. Often unable to reach the river channel, the caiman fast until the flood of the next rainy season fills the ponds and fish move back into the pods from the river channel.

Many other ectotherm sauropsids tolerate fasting intervals of several months (Wang et al., 2006; McCue, 2007); but, when they feed, they consume a wide range of meal sizes, which in the extreme may exceed their own body mass (Pope, 1961; Green, 1997). Shortly after feeding, the metabolic rate, the activity of digestive enzymes increase, and, in some species, the activity of mucosal membrane nutrient transporters also increases. Such postprandial response is associated with an increase of organ size of the gastrointestinal system. Patterns and processes of the postprandial response have been predominantly studied in snakes (Secor et al., 1994; Secor and Diamond, 1995; Starck and Beese, 2001; Overgaard et al., 2002; Starck and Beese, 2002; Starck, 2005). For snakes, the postprandial size increase of the small intestine, in particular the increase of the absorptive area, involves a configuration change of the mucosa epithelium from pseudostratified to single layered and an hypertrophy of enterocytes due in part to the incorporation of lipid droplets (Starck and Beese, 2001; Starck and Beese, 2002; Lignot et al., 2005; Starck, 2005; Starck and Wimmer, 2005). A larger blood flow volume directed to the gut during digestion has also been shown to contribute to increasing organ size, possibly as a hydraulic pump that inflates the villi (Starck and Wimmer, 2005). The size increase of the liver is based on incorporation of lipid droplets into hepatocytes and

increased blood flow volume (Starck and Beese, 2001; Starck and Beese, 2002; Starck, 2005; Starck and Wimmer, 2005). The same histological patterns associated with the postprandial size changes of the gut have been described in three frog species (Cramp, 2005; Cramp and Franklin, 2005; Cramp et al., 2005; Starck, 2005). Although only little information is available yet, these histological patterns that have been observed during the postprandial response of ectotherm sauropsids and anurans differ from those processes that drive the organ size changes in birds and mammals, observed after diet shifts or during fasting. In birds and mammals, the size changes of the small intestine are primarily based on cell proliferation during size increase, and epithelial cell loss during decreasing size (Konarzewski and Starck, 2000; Dunel-Erb et al., 2001; Starck, 2003; Habold et al., 2004; Karasov et al., 2004; Starck, 2005). Enterocytes may also experience some degree of hypertrophy when changing from fasting to fed condition in mammals. The magnitude of the functional responses to feeding for amphibians and reptiles has been proposed to be adaptively correlated with feeding habits, i.e. species that experience long episodes of fasting regulate intestinal performance over a wider range than more frequently feeding species (Secor et al., 1994; Secor and Diamond, 1998; Secor, 2001). So far, phylogenetic comparisons consider primarily physiological and cross morphological responses to feeding (Secor and Diamond, 2000; Secor, 2005b; Secor, 2005a). From a histological and comparative perspective, the more recent data from frogs suggest that the postprandial patterns of gastrointestinal size increase might be a plesiomorphic feature shared by all tetrapods, with birds and mammals showing derived patterns of organ size changes.

We cannot test this hypothesis for tetrapods but, here, take a more focused view on sauropsids. Within the sauropsids, birds and squamates represent a phylogenetic bracket to crocodiles with crocodiles being the sister group to birds. Thus crocodiles take a pivotal phylogenetic position for any comparative analysis of the evolution of organ response. If crocodilians show the same pattern of change on the level of cells and tissue as described for other ectotherm sauropsids, the most parsimonious interpretation will be that this pattern is plesiomorphic for tetrapods, and that birds and mammals evolved independent mechanisms of organ size changes. In this study, we therefore aimed at: (1) a detailed characterization of the postprandial response of oxygen consumption, organ size change, and structural changes on the level of tissues and cells in a crocodilian species to understand how this species adjusts to periods of feeding and fasting; and (2) contributing comparative histological and cytological data to understand better the evolutionary history of organ size changes in sauropsids.

## Materials and methods

### *Animals*

Broad nosed caimans *Caiman latirostris* (Daudin 1801), were raised in the Jacarezário at the State University of São Paulo in Rio Claro, Brazil (25°46′60″S; 53°45′0″W). For repeated ultrasonography, 15 two-year-old individuals (body mass range 3.6–5.4 kg, mean 4.1±0.65 kg) and 15 three-year-old caimans (body mass range 8.0–18.0 kg, mean 13.5±3.7 kg) were chosen randomly from the group of available animals. Animals were housed in 12×10 m outdoor enclosures. Each enclosure had a 2×1.5×10 m pool, free access to dry resting places and to shade places. All animals were exposed to the natural daily temperature regime (mean temp. 21.9°C, range 27.3–18.1°C), humidity (mean relative humidity 70%), and photoperiod (13 h:11 h, L:D). For respirometry, we used a group of eight one-year-old individuals (body mass range 1.4–1.9 kg, mean 1.68±0.38 kg). Those animals were housed in rearing pens of 1.2×1.2 m dimensions.

### *Experimental setup and feeding regime*

#### *Ultrasonography*

Animals were assigned to two groups of 15 animals each. The three-year-old caimans were fasted for 3 months while the 2-year-old caimans were fed a small amount of food (chicken necks, <1% of body mass) every 3 days during the same period of time. After this period, ultrasonographs were taken every 3 days for 2 weeks to document the dimensions of the small intestine and liver during fasting and feeding. After 2 weeks of ultrasonography, the fasting animals received a single meal (chicken necks) between 5% and 10% of the individuals' body mass. After feeding, ultrasonography was continued with the same schedule for 2 more weeks to observe organ size changes in response to feeding. The feeding group experienced the same 2-week period of ultrasound-scanning while being fed every 3 days. Following this 2-week period, fed animals were fasted and we continued to monitor organ size using ultrasound, now in response to fasting. Two types of comparisons were made (i) within each group (longitudinal comparisons), and (ii) between groups.

#### *Respirometry*

Eight one-year-old individuals were randomly chosen from the available animals. These animals had been fasting for at least 1 week before measurements began. To measure oxygen consumption, we used closed system respirometry over a period of 12 days (details see below). The animals were fed (chicken necks) on day 3 of metabolic measurements. The amount of food was between 7% and 15% of the individuals' body mass (mean 11.5±2.7%).

### *Ultrasonography*

We used a portable Sonosite 180plus ultrasonography system (Sonosite Inc., Bothel, WA, USA) equipped with a 5–10 MHz broadband linear array transducer for B-image ultrasonography. The spatial resolution of the system is <0.02 mm. The caimans were scanned in the laboratory to avoid overheating of the animals during ultrasound scanning. We used ultrasound gel to couple the scanner head to the skin. Ultrasonography sessions were recorded on digital video, and still images for morphometry of organ size were later extracted from video tapes. The liver and the small intestine of 30 caimans were

scanned every third day during fasting and after feeding. All experiments were performed at the Jacarezário of the State University of São Paulo in Rio Claro, Brazil. Histology and morphometry were conducted at the LMU, Munich, Germany.

### *Ultrasonographic morphometry and statistics*

From video recordings we extracted still images at 760×840 pixel resolution. We recorded a minimum of five images each of the liver, the duodenum and the distal small intestine for each animal at each recording session. From ultrasonographs, we measured the thickness of the mucosa of the duodenum, the thickness of the mucosa of the distal small intestine, and the cross section of the liver (see below for morphological landmarks). From the mucosa of the duodenum and the distal small intestine we took multiple measurements, whereas we took only one measurement from the liver cross section. We used SigmaScan v. 5.0 (Jandel Sci., SPSS Inc., Chicago, IL, USA) as the morphometry program. For statistics, we calculated daily means for each individual from multiple morphometric measurements. None of the variables differed from normal distribution. To test between groups for the effect of feeding and the day after feeding we used repeated measures analysis of covariance (RM-ANCOVA). 'Feeding group' was the inter-subject factor, 'day after feeding' was the within-subject factor, and body mass was the covariate. When body mass was significant as the covariate, estimated least square means (LS means) ± s.e.m. are given in the text and figures to exclude the effect of body mass; raw data are summarized in Appendix 1. To analyze in more detail the effects of day after feeding within each group of caimans, we first tested data with a univariate ANCOVA with body mass a covariate and day after feeding as main effect. When body mass was not significant as a covariate, we repeated the analysis as a univariate ANOVA followed by Tukey's HSD *post-hoc* comparison of multiple means to analyze for differences between days after feeding. SPSS v. 12.01 (SPSS Inc., Chicago, IL, USA) was used for all statistical analyses.

### *Dissections and histology*

Five animals that had been fasting for 3 months and five digesting animals were killed by an overdose of pentobarbital (Nembutal; Beyer, Leverkusen, Germany). Immediately following, a midventral incision was made to expose the body cavity, body condition was inspected, and the liver and small intestines were removed and weighed using a laboratory scale (precision 0.01 g). Tissue samples of the duodenum, the small intestine and liver were preserved for histology in 5% paraformaldehyde in 0.1 mol $l^{-1}$ phosphate buffer at pH 7.4 and 4°C for at least 48 h. They were then washed in buffer, dehydrated through a graded series of ethanol to 96% ethanol and embedded in hydroxyethyl methacrylate (Historesin, Fa. Leica, Germany). Embedded material was sectioned into a short series of 50 sections per sample (section thickness was 2 μm), mounted on slides and stained with Methylene Blue–Thionin. Histological sections were studied using a Zeiss Axioplan microscope equipped with a digital camera (Canon Powershot 80) and connected to the image-analysis and morphometry computer system. Photomicrographs were taken with the digital camera. An additional set of tissue samples for electron microscopy were preserved in 2.5% glutaraldehyde in 0.1 mol $l^{-1}$ phosphate buffer at pH 7.4 and 4°C for at least 48 h, then washed in buffer, postfixed in 1% osmium tetroxide for 30 min, dehydrated through a graded series of ethanol and then embedded in Durcopan ACM resin (Sigma/Fluka, Munich, Germany) following standard protocols. We used a CM10 transmission electron microscope (Phillips, Munich, Germany) to examine the specimens.

### *Histological morphometry*

For the proximal and distal small intestine, we measured the thickness of the muscle layer at three sites for each of ten cross sections per animals. The thickness of the muscle layer (tunica muscularis) was measured as a straight line from the inner to the outer margin of the muscle layer. The epithelial surface magnification was measured as the epithelial surface over a baseline defined by the inner circular muscle layer. Measurements were made by tracing the epithelial surface with a cursor on a digitizing tablet and calculating its total length divided by the length of the baseline, expressed as a dimensionless ratio. For each animal an average value from multiple measurements was calculated to avoid pseudoreplication of data. We used one-factor ANCOVA with feeding as factor and body mass as covariate for statistical analysis.

Although fixation of tissue in isotonic and buffered paraformaldehyde, dehydration to 96% ethanol and embedding in methacrylate minimizes embedding artefacts, the procedure may result in about 10% shrinkage of tissue as compared to the original size (Böck, 1989). However, all tissue samples were treated identically thus can be compared directly.

### *Respirometry*

We used a Sable Systems $O_2$ analyzer, model PA-1 (Sable Systems, Las Vegas, NV, USA) connected with a Sable Systems multiplexer with eight parallel metabolic chambers (chamber volume 15 l) to measure oxygen consumption. The system was set up so that oxygen content in one chamber was recorded in a closed circuit for 10 min while the other chambers were ventilated. After 10 min the system automatically switched to the next chamber. The metabolic chambers were placed in a constant-temperature cabinet at 30°C with an automated 12 h:12 h L:D photoperiod. The air stream that was vented from the metabolic chamber to the $O_2$ analyzer was dried with silica gel before entering the oxygen analyzer. Each day, measurements were interrupted between 10:00 h and 12:00 h to rehydrate the animals. Oxygen consumption was calculated as:

$$\dot{V}_{O_2} = \left[ \frac{(V_{chamber} - V_{caiman})\,(F_{startO_2} - F_{endO_2})}{F_{startO_2}} \right] / t \,,$$

where $\dot{V}_{O_2}$ is oxygen consumption (ml $g^{-1}$ $h^{-1}$), $V_{chamber}$ is the

volume of the respiratory chamber (in ml), $V_{caiman}$ is the volume of the caiman (calculated as caiman mass in grams × 1.01 ml $g^{-1}$) (Peterson, 1990), $F_{startO_2}$ and $F_{endO_2}$ are oxygen concentrations measured at the beginning and the end of the experiment, respectively, and $t$ is the time of measurement (Vleck, 1987; Cullum, 1997). The specific dynamic action was calculated by fitting a log-normal four-parameter model to the $\dot{V}_{O_2}$ data using nonlinear regression and then integrating the area under the curve from the day of feeding to the day after feeding when metabolic measurements were not significantly different from standard metabolic rate (SMR), minus energy investment for SMR during that period. SMR was calculated as the average of 3 days of mass specific oxygen consumption from fasting animals. Form this value we calculated daily energy expenditure in SMR for an average animal of 1.68 kg body mass. We used a conversion factor of 19.8 J $ml^{-1}$ $O_2$ consumed (Secor, 2001).

## Results

During dissection, all caimans were inspected for the thickness of their peritoneal adipose tissue and the size of the pelvic adipose body. All caimans possessed peritoneal adipose pads between 1 and 5 cm in thickness. The thickness of the pelvic adipose body was between 5 cm and 10 cm in all animals. Obviously, body condition was excellent even after 3 months of fasting.

Even though caimans fasted for 3 months were on average larger and older ($N$=5; mean body mass, 11.6±4.3 kg), wet mass of the small intestine (84.95±35.1 g) was significantly less than that of caimans that fed continuously ($N$=5; mean post-absorptive body mass, 5.2±0.8 kg; small intestine fresh mass 94.4±23.3 g). To account for the effect of body mass we calculated least square means for small intestine fresh mass. Those were 61.85±11.99 g for fasting caimans and 117.52±11.99 g for digesting caimans (ANCOVA with body mass as covariate, d.f.=2,1; $F$=7.72; $P$=0.027 for fasting *versus* feeding, body mass was significant as a covariate d.f.=2,1; $F$=9.36; $P$=0.018).

Body mass had a considerable effect on liver fresh mass (fasting caimans, 121.2±61 g; digesting caimans 92.9±19.6 g). However, when the effect of body mass was excluded the mass of the liver differed significantly between fasting and digesting caimans. Least square means of the liver of fasting caimans was 76.67±9.1 g and 137.39±9.1 g for digesting caimans (ANCOVA with body mass as covariate, d.f.=2,1; $F$=15.94; $P$=0.005 for fasting *vs* feeding, body mass was significant as a covariate d.f.=2,1; $F$=60.31; $P$<0.001).

### *Ultrasound imaging and morphometry*

Morphometry based on ultrasonography requires clearly defined scanner head positions and morphological landmarks that warrant repeatable image contents. The chessboard pattern of the scales on the caiman's belly provides a natural grid for reproducible external scanner head positions (Fig. 1A). For small individuals, the ossification of the ventral scales did not matter but for large individuals (<170 cm) the scanner head had to be positioned between scales to allow ultrasound access.

The duodenum emerges directly from the stomach and forms a U-shaped loop next to the caudal margin of the right liver lobe and ventral to the gall bladder (Fig. 1B). Anatomically it is characterized by the pancreas located between ascending and descending loop of the duodenum, by multiple entrances of ducts from pancreas, gall bladder, and liver. Ultrasonography access to the duodenum is from the ventral right side of the belly (Fig. 1A). The duodenum can be recognized as that part of the small intestine located immediately caudal to the gall bladder (Fig. 1C). Positioning of the ultrasound scanner head as shown in Fig. 1A will result in two cross sections through the duodenal loop (Fig. 1C). Distal loops of the small intestine are seen when the scanner head is placed on the right side of the belly in a more lateral and horizontal position. A typical and easily reproducible ultrasonograph is shown in Fig. 1D with four cross sections through loops of the distal small intestine and a longitudinal section below the cross sections. The liver can be accessed by ultrasound from the right side (Fig. 1A). As landmarks for the scanner head position, we defined the gall bladder (right side of image), a cross section of the liver portal vein and the distal tip of the liver (Fig. 1E).

### *Size changes of the duodenum*

In caimans fasting for 3 months, the thickness of the duodenal mucosa was on average 5.38±0.44 mm (LS means ± s.e.m. $N$=15 animals, each individual measured twice after a 3-month fast; Fig. 2). Within 3 days after feeding, the thickness of the mucosa doubled to 10.58±0.56 mm (LS means ± s.e.m., $N$=15). During the following 9 days, the mucosa thinned continuously and by day 12 post feeding mucosal thickness (7.05 mm; $N$=8) did not differ from that when fasting. For caimans fed continuously, the thickness of the duodenal mucosa ranged between 6.2±0.44 and 8.1±0.51 mm (LS means ± s.e.m., $N$=15; Fig. 2). When feeding was interrupted, mucosal thickness declined to 5.8±0.56 mm (LS means ± s.e.m., $N$=9). We first used an RM-ANCOVA to test for differences between both groups (see Materials and methods). 'Feeding group' and 'day after feeding' combined produced a highly significant effect on duodenal mucosa thickness (d.f.=9,173; $F$=9.9; $P$<0.001). Body mass was significant as a covariate (d.f.=1,173; $F$=13.76; $P$=0.013). In a second analysis, we tested the effects of 'day after feeding' within each group of caimans (longitudinal comparison). In the caimans, that were first fasted and then fed a single meal, the duodenal mucosa was significantly thicker 3 days after feeding (Table 1). Mucosal thickness declined slowly. Nine days after feeding the thickness of the mucosa in this group could not be distinguished statistically from the fasting group. In the caimans that had been feeding for 3 months and then fasted, significant differences in the thickness of the duodenal mucosa were observed 9 days after feeding was interrupted (Table 1).

The same general pattern of changes in mucosal thickness was found in the distal small intestine (Fig. 3). The combined

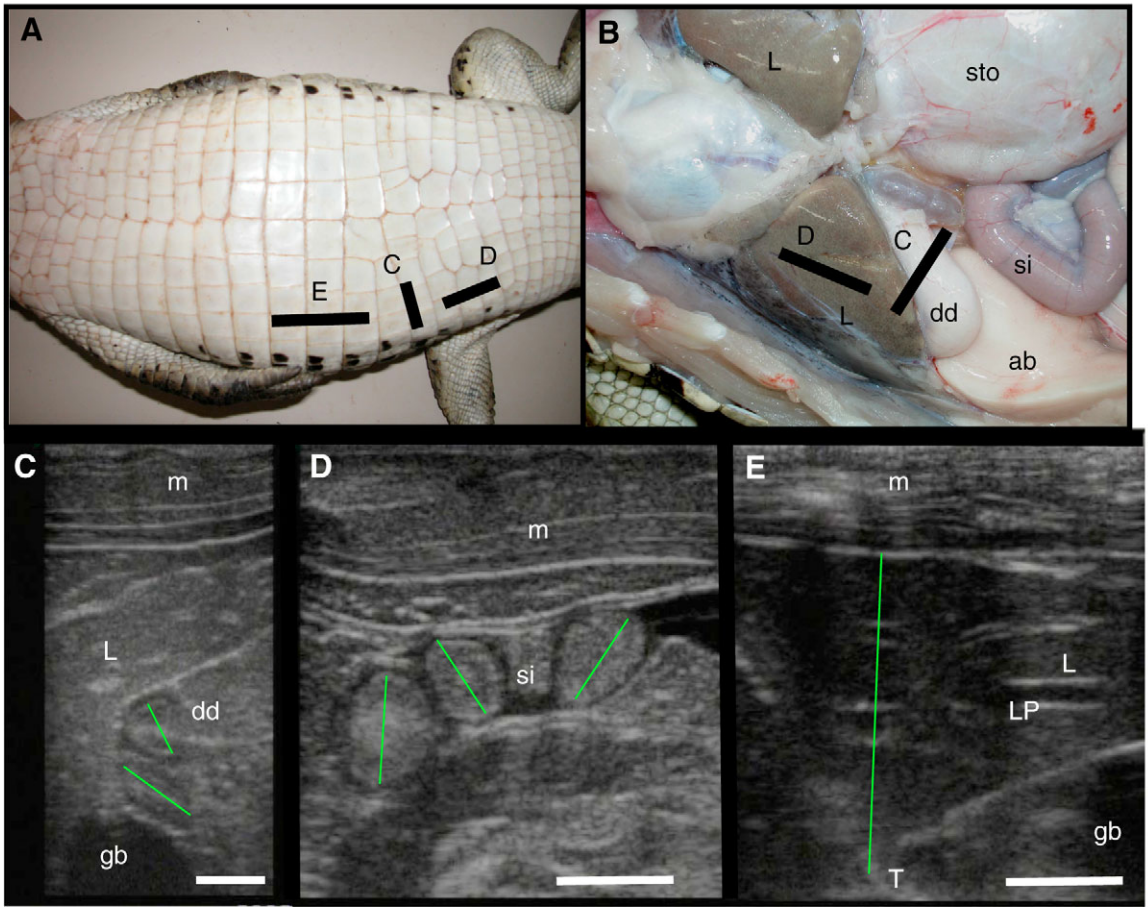


Fig. 1. Anatomy and ultrasonography of broad nosed caiman. (A) Chequerboard pattern of ventral scales and marks for application of the ultrasound scanner head (B) Partial situs of the body cavity. Black bars in A and B indicate scanner head position resulting in the images in C, D and E; (C) duodenum and liver (D). (C–E) Ultrasound anatomy of the duodenum (C), distal small intestine (D), and liver and gall bladder (E). Ultrasound anatomy of the liver and gall bladder. Abbreviations: ab, adipose tissue body; dd, duodenum; gb, gall bladder; L, liver; m, ventral muscles; si, distal small intestine; sto, stomach. The scanner head was positioned on the ventral scales of the caiman, thus in the ultrasonographs (C–E) ventral is at the top and dorsal is at the bottom. Green lines in C–E indicate the morphometric measurements. Scale bars, 1 cm (C–E).

effects of feeding group and day after feeding had a highly significant effect (d.f.=9,166; $F$=4.64; $P$<0.001) on mucosal thickness of the small intestine. Body mass was significant as a covariate (d.f.=1,166; $F$=26.46; $P$<0.001). In the group of caimans that was fasted for 3 months and the fed a single meal (longitudinal comparison), we observed statistically significant doubling of the thickness of the small intestinal mucosa epithelium within 3 days after feeding. Nine days after the size peaked, the mucosal thickness had declined to values that were not different from those in fasting caimans (Table 1). The observed fluctuations in mucosal thickness after day 15 in the experiment were statistically not significant. The caimans that had been fed during the 3 months, had a thicker mucosa than the fasted caimans. However, when feeding was interrupted, the thickness of the small intestinal mucosa epithelium

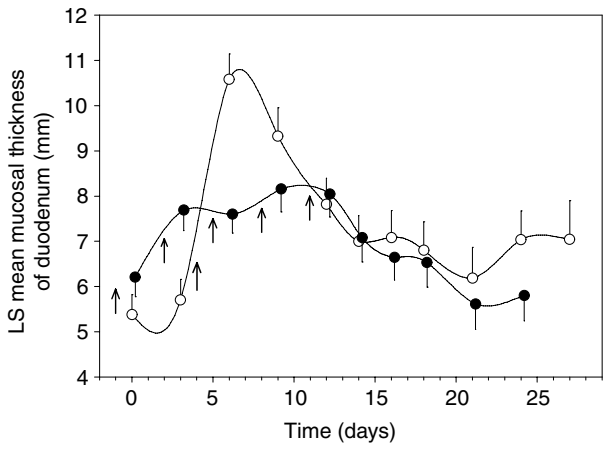


Fig. 2. Changes in the thickness of the mucosa in the duodenum as measured by ultrasonography. Black symbols with negative error bars represent values from caimans that were first feed then fasted, white symbols with positive error bars are values from caimans fasted for 3 months then feed a single meal. Values are least square means ± s.e.m. derived from RM ANCOVA; for raw data see Table 1. Arrows indicate feeding events for each experimental group.

Table 1. *Body mass, morphological response variable and sample size for the two experimental groups of caimans*

| Day | Body mass | Duodenum | Small intestine | Liver | *N* |
|---|---|---|---|---|---|
| Feeding | | | | | |
| 0 | 4.5±0.65 | 5.8±1.75$^{a,b,c}$ | 5.7±1.81$^{a,b,c,d}$ | 21.4±3.74 | 15 |
| 3 | 4.5±0.65 | 7.2±1.74$^{b,c}$ | 7.0±1.83$^{c,d}$ | 21.0±5.16 | 15 |
| 6 | 4.5±0.65 | 7.1±1.70$^{a,b,c}$ | 7.3±1.32$^{d}$ | 27.3±7.18 | 15 |
| 9 | 4.5±0.65 | 7.7±1.81$^{c}$ | 7.2±0.86$^{d}$ | 27.9±4.26 | 15 |
| 12 | 4.3±0.36 | 7.6±1.73$^{c}$ | 6.7±1.59$^{b,c,d}$ | 27.3±4.75 | 11 |
| 14 | 4.3±0.42 | 6.6±1.29$^{a,b,c}$ | 5.1±0.64$^{a,b}$ | 24.7±3.47 | 11 |
| 16 | 4.3±0.56 | 6.2±0.71$^{a,b,c}$ | 5.2±0.48$^{a,b,c}$ | 24.8±1.45 | 9 |
| 18 | 3.7±0.63 | 6.0±0.71$^{a,b,c}$ | 5.0±0.95$^{a,b}$ | 24.1±5.85 | 9 |
| 21 | 4.2±0.46 | 5.1±0.58$^{a}$ | 4.8±0.83$^{a}$ | 26.7±5.94 | 9 |
| 24 | 4.3±0.45 | 5.3±0.80$^{a,b}$ | 5.1±0.51$^{a,b}$ | 25.3±3.03 | 9 |
| Fasting | | | | | |
| 0 | 13.5±3.69 | 5.9±1.47$^{a}$ | 5.3±1.19$^{a}$ | 28.4±7.46 | 15 |
| 3 | 13.5±3.69 | 6.2±1.02$^{a}$ | 6.7±1.67$^{a,b}$ | 35.8±6.64 | 15 |
| 6 | 13.2±3.67 | 11.1±2.19$^{c}$ | 10.7±0.99$^{c}$ | 36.1±5.12 | 14 |
| 9 | 15.9±3.56 | 10.3±2.27$^{b,c}$ | 10.1±1.59$^{b,c}$ | 39.6±6.91 | 11 |
| 12 | 14.4±3.54 | 8.4±1.60$^{a,b,c}$ | 8.5±1.21$^{a,b,c}$ | 37.2±6.10 | 9 |
| 14 | 12.8±3.70 | 7.6±1.18$^{a,b}$ | 6.8±1.87$^{a,b}$ | 36.6±9.11 | 9 |
| 16 | 14.6±2.49 | 7.6±1.19$^{a,b}$ | 7.5±2.54$^{a,b,c}$ | 29.3±6.68 | 8 |
| 18 | 15.1±3.83 | 7.5±1.40$^{a}$ | 6.7±1.92$^{a,b}$ | 31.4±4.76 | 9 |
| 21 | 13.3±3.65 | 6.6±1.29$^{a,b}$ | – | 29.9±9.10 | 7 |
| 24 | 13.3±3.92 | 7.5±1.85$^{a}$ | 7.4±2.03$^{a,b,c}$ | 28.1±4.55 | 7 |

Values are mean ± s.d. of body mass, thickness of the duodenal mucosa, thickness of the small intestinal mucosa, and liver size when measured with ultrasonography. Within each group, values denoted by different letters differ significantly according to Tukey's HSD *post hoc* test for comparison of multiple means, $\alpha<0.05$.

declined, reaching significantly different values 6 days after feeding stopped (Table 1).

Size changes of the liver (Fig. 4) were not as clear as in duodenum and distal small intestine. In a RM-ANCOVA with feeding group as inter-subject factor, day after feeding as within-subjects factor and body mass as covariate, feeding group (d.f.=1,4289; $F$=1.69; $P$=0.212) and day after feeding (d.f.=9,8.99; $F$=1.24; $P$=0.376) were not significant. However, the combined effects of feeding group and day after feeding were significant (d.f.=9,167; $F$=2.67; $P$=0.003) on liver size.

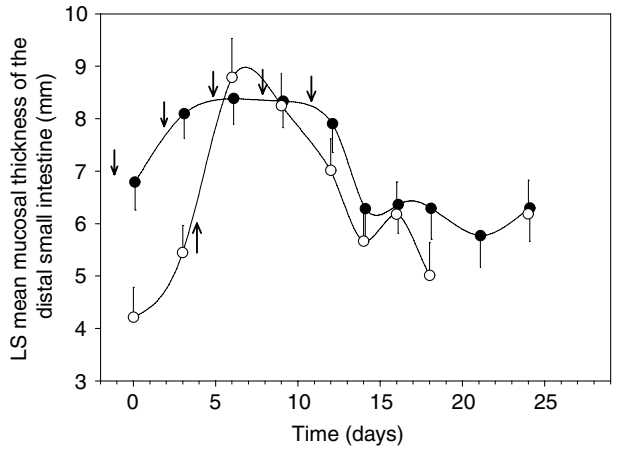


Fig. 3. Changes in the thickness of the mucosa in the distal small intestine as measured by ultrasonography. Black symbols with negative error bars represent values from caimans that were first feed then fasted, white symbols with positive error bars are values from caimans fasted for 3 months then feed a single meal. Values are least square means ± s.e.m. derived from RM ANCOVA; for raw data see Table 1. Arrows indicate feeding events for each experimental group.

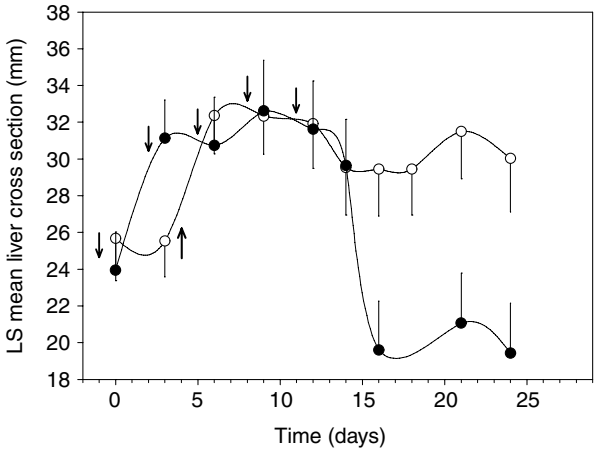


Fig. 4. Changes of the size of the liver as measured by ultrasonography. Black symbols with negative error bars represent values from caimans that were first feed then fasted, white symbols with positive error bars are values from caimans fasted for 3 months then feed a single meal. Values are least square means ± s.e.m. derived from RM ANCOVA; for raw data see Table 1. Arrows indicate feeding events for each experimental group.

Body mass was significant as a covariate (d.f.=1,167; $F$=25.96; $P$<0.001). When comparisons were made within groups between days after feeding, the observed size changes of the liver in caimans that were fasting and then fed a single meal were not significant. Caimans that were first fed then fasted showed a decline in liver size when feeding was interrupted. However, that decline was not significant (Table 1).

*Light microscopy and transmission electron microscopy*

Light microscopy (LM) of the mucosa epithelium of the duodenum and the small intestine showed distinct differences in the fasting and digesting groups. When digesting, the mucosa epithelium was a single layered, columnar epithelium with a prominent brush border. The enterocytes were relatively narrow, rarely being wider than the nucleus. The cytoplasm of the enterocytes was filled with lipid droplets (Fig. 5A,B). At many positions along the epithelium, the apical end of the enterocytes was swollen, most certainly due to the loading of the cells with lipid droplets. The nuclei of the enterocytes were positioned basally or medially. If only the apical part of the cell was filled with lipid droplets, then the nuclei were located basally, if droplets had already been transported to the basal part of the cell then the nuclei become shifted more medially (compare Fig. 5A and B). Paracellular spaces were found between the basal parts of the enterocytes. Transmission electron microscopy (TEM) of the apical border of the enterocytes showed long microvilli, and a well developed terminal web, which was recognizable as a layer of electron dense material (Fig. 5D,E). The basal roots of the actin filament cytoskeleton of the microvilli ended in the terminal web. The cell membrane between the roots of the microvilli showed numerous pinocytotic membrane inclusions (Fig. 5E), which develop during lipid absorption and supposedly are precursors of membrane-coated transport vesicles in the enterocyte cytoplasm (Ashworth and Lawrence, 1966). Throughout the cytoplasm of active enterocytes, we observed a large number of mitochondria with well developed cristae. In addition, a number of electron dense vesicles were found, which presumably were lysosomes. We observed topographic differences in the morphology of the enterocytes along the length of a villus. In particular, the enterocytes at the tip of the villi were enlarged and appeared to be overloaded with lipid droplets (Fig. 5C) whereas enterocytes at the base of a villus contained fewer lipid droplets. Some of the enterocytes at the tip of the villi showed clear signs of necrosis, i.e. swollen cell body, lysis of the cytoplasm, structural dissociation of the cell and breakdown of the cell membrane. Of course, histological studies cannot reveal the mechanisms underlying necrosis of cells, but we assume that necrosis was related to overloading of enterocytes with lipid droplets. Only a few goblet cells were found in the duodenal and small intestinal mucosa epithelium, but, a large number of intraepithelial lymphocytes were found throughout the epithelium, some close to the basement membrane, and others next to the brush border. We have not attempted to quantify immune cell numbers, but inspection of a series of histological slides showed that lymphocytes are most numerous close to the base of the intestinal villi, where they appear to emerge from lymphatic aggregations. From there, they migrate along the basal membrane to the tip of the villi. Along this cellular traffic route, lymphocytes penetrate the basal membrane and integrate into the mucosa epithelium.

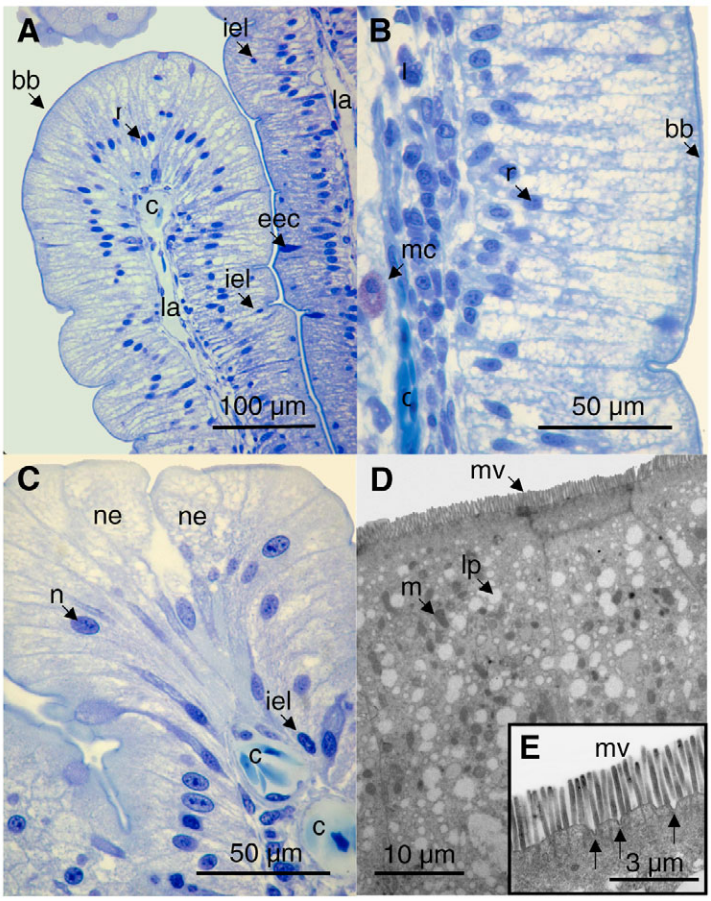


Fig. 5. Light microscopy and transmission electron microscopy of the duodenal mucosa epithelium of digesting caimans. Enterocytes are filled with lipid droplets and arranged as a single layered high prismatic epithelium. (A) Low power light micrograph of a villus showing the typical arrangement of lipid filled enterocytes with a well developed brush border and a large capillary in the connective tissue core of the villus. (B) High power light micrograph of the mucosa epithelium. Note the dense layer of lyphocytes and a large mast cell below the epithelium. (C) High power light micrograph of the tip of a villus with necrotic cells. Necrotic cells are enlarged as compared with healthy enterocytes and show different degrees of lysis of the cell membranes as well as the nuclei. (D) Low power transmission electron micrograph. Note the dense distribution of mitochondria and lipid droplets. (E) High power transmission electron micrograph of the brush border with pinocytotic pits at the basis of microvilli (arrows). bb, brush border; c, capillary; eec, enteroendocrine cell; iel, intraepithelial lymphocyte; l, lymphocytes; la, lacteal; lp, lipid droplet; m, mitochondria; mc, mast cell; mv, microvilli; n, nucleus of enterocytes; ne, necrotic enterocytes.

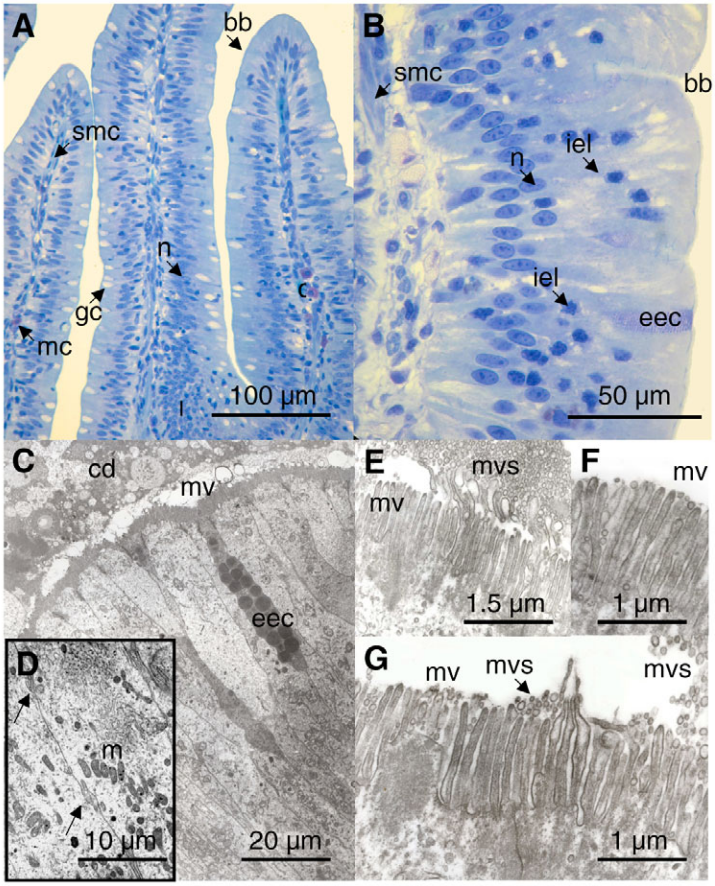


Fig. 6. Light microscopy and transmission electron microscopy of the duodenal mucosa epithelium of fasting caimans. The enterocytes are narrow, contain no lipid droplets, and are arranged as a pseudostratified epithelium. The brush border is barely visible. The connective tissue cores of the villi are broader and more condensed than in digesting caimans. (A) Low power light micrograph, showing the arrangement of arrangement of the enterocytes as typical pseudostratified epithelium. Note the aggregation of lymphocytes at the base of the middle villus. (B) High power light micrograph of the mucosa epithelium (same magnification as Fig. 5B). (C) Transmission electron micrograph of the mucosa epithelium with enterocytes and one enteroendocrine cell, the lumen of the gut contains an accumulation of cellular debris. (D) Segment of the cell membrane of two adjoining enterocytes showing folds of spare membrane (arrows). (E) Microvilli of an enterocyte exfoliating membrane vesicles from the tip of the microvilli. (F) Bifurcating microvilli. (G) Microvilli of the brush border disintegration, i.e. swollen tips and formation of membrane vesicles. bb, brush border; cd, cellular debris in lumen of gut; eec, enteroendocrine cell; gc, goblet cell; iel, intraepithelial lymphocyte; l, lymphocytes; m, mitochondria; mc, mast cell; mv, microvilli; mvs, membrane vesicles; n, nucleus of enterocytes; smc, smooth muscle cell.

Large mast cells were located below the basal membrane of the epithelium (Fig. 5B). In digesting caimans, the lamina propria mucosae (i.e. the connective tissue core of a villus) was narrow, capillaries and lymphatic vessels were large and easily recognizable. The smooth muscle fibers were thin and appear stretched (Fig. 5A).

When fasting, the mucosa epithelium had a different configuration. Most noticeably, the enterocytes contained no lipid droplets and no paracellular spaces were found (Fig. 6A–C). Under LM, the brush border was barely visible and the terminal web could not be recognized. The nuclei and cytoplasmic bodies of the enterocytes were arranged in several layers whereas their bases were attached to the basal membrane. This particular cellular configuration results in the appearance of a typical pseudostratified epithelium. A few goblet cells could also be seen interspersed in the epithelium. Enterocytes at the tip of the villi were not necrotic. Along the length of a villus, most of the lymphocytes and mast cells were lined up below the basal membrane of the epithelium, i.e., only few lymphatic cells had integrated into the epithelium. The lamina propria mucosae was much more condensed, and capillaries and lymphatic vessels were much smaller than in digesting caimans (Fig. 6A). In TEM images, the lateral cell membrane of neighboring enterocytes showed folds of spare membrane which were not found in active enterocytes. These folds of spare membrane were found throughout the epithelium of fasting animals. At the apical end of the enterocytes, the terminal web was not as prominent as it was in active enterocytes and the microvilli were short and stout, some showing bifurcations (Fig. 6E). No pinocytotic pits were found between the microvilli. The microvilli of many enterocytes showed clear signs of lysis (Fig. 6D–F), apparent as a lack of the actin filament skeleton within the microvilli, the enlarged tips of microvilli, and the numerous membrane vesicles that had formed at the tip of the villi. Those membrane vesicles dissociated from the microvilli and were discharged into the lumen of the gut. The length of the microvilli varied along a villus. Therefore, the methods used and without a reproducible marker for the position of enterocytes on the villus we could not quantify the length of the microvilli. However, as a general impression it appears that in fasting animals the microvilli are shorter and the actin filaments of the microvilli reach deeper into the cytoplasm than they do in digesting animals. This suggests that length changes of the microvilli may be accomplished by an actin filament mechanism that simply pushes microvilli back and forth (Secor, 2005a).

Histological morphometry identified highly significant differences in the size of the absorptive surface of fasting and digesting caimans. The absorptive surface of the mucosa epithelium in the duodenum of digesting caimans was significantly larger (univariate ANCOVA; feeding group as main effect; d.f.=1,10; $F$=6.347; $P$=0.036; body mass as covariate was not significant; Fig. 7) and the distal small intestine (univariate ANCOVA; feeding group as main effect;

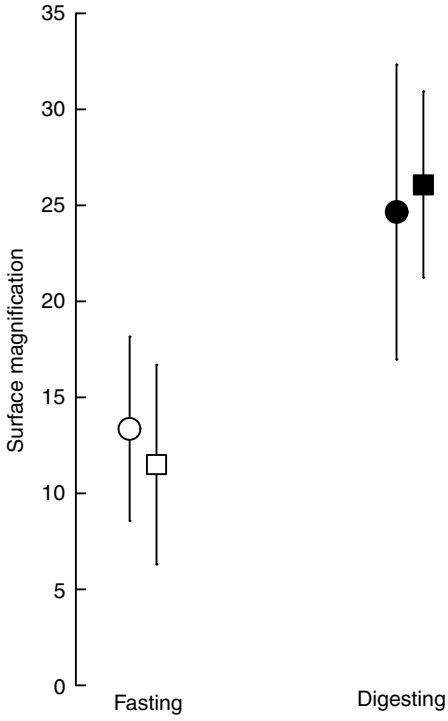


Fig. 7. Changes in the absorptive surface of the duodenum (circles) and the small intestine (squares) in feeding (filled symbols) and fasting (open symbols) caimans. Values are means ± s.d. from *N*=5 animals. Differences between the feeding and fasting condition are highly significant (see text for details of statistics).

d.f.=1,5; $F$=13.60; $P$=0.01; body mass as covariate was not significant; Fig. 7). Digesting and fasting caimans did not show differences in the thickness of the muscle layer of the duodenum (feeding: 1.1±0.12 mm; fasting 1.2±0.3 mm) or the distal small intestine (feeding 1.2±0.12 mm; fasting 1.3±0.18 mm).

Light microscopy of the liver showed the typical tubular structure and zonal arrangement of hepatocytes. Periportal fields containing branches of the hepatic artery, the vena portae hepatica, and bile ducts were found throughout the parenchyma. However, because the liver parenchyma of crocodiles is not a lobular structure, as is characteristic of mammalian liver, the periportal fields cannot easily be associated with the functional units of a liver acinus (Fig. 8). Sinusoids are very narrow and, due to the lack of a lobes, appear less organized than in the mammalian liver. Numerous Kupffer cells were dispersed throughout the liver parenchyma. Although fat-storing cells (stellate cells) have been described as components of the perisinusoidal space in the crocodilian liver (Storch et al., 1989), light microscopy and the considerable loading of hepatocytes with lipid droplets meant that it was not possible to identify this type of cell. The hepatocytes of feeding and fasting caimans were loaded with numerous lipid droplets. Fig. 8C,D shows the typical zonal arrangement, with the nuclei of the hepatocytes close to the base and the lipid droplets filling the apical part of the cell body. Lipid storage in hepatocytes is a normal condition in sauropsids (Storch et al., 1989; Schaffner, 1998; Ganser et al., 2003). Although the histology showed similarities with mammalian microvesicular hepatosteatosis, the condition in crocodiles is healthy and must not be confused with the pathological condition of the mammalian liver. No differences in liver structure of fasting and feeding caimans could be detected with light microscopy. Obviously, even those caimans fasting for 3 months were still in a body condition in which hepatocytes were loaded with lipid droplets. This observation is important in interpretation of the lack of observable size changes of the liver.

### *Respirometry*

Oxygen consumption ($\dot{V}_{O_2}$) of eight juvenile caimans was measured continuously over a period of 12 days, starting 3 days before feeding (Fig. 9A). The mass-specific $\dot{V}_{O_2}$ of fasting caimans was 0.016±0.002 ml $O_2$ $g^{-1}$ $h^{-1}$ (average of 3 days consumption for eight animals) and we calculated daily energy expenditure in SMR as 12.83 kJ $day^{-1}$ for an average animal of 1.68 kg body mass. On the feeding day, respirometry was interrupted for 5 h for feeding of the animals. When respirometry measurements resumed after feeding $\dot{V}_{O_2}$ had already increased, reaching peak values 24–48 h after feeding (Fig. 9A) at an average of 0.026± 0.022 ml $O_2$ $g^{-1}$ $h^{-1}$. Thereafter, $\dot{V}_{O_2}$ declined constantly, returning to fasting values

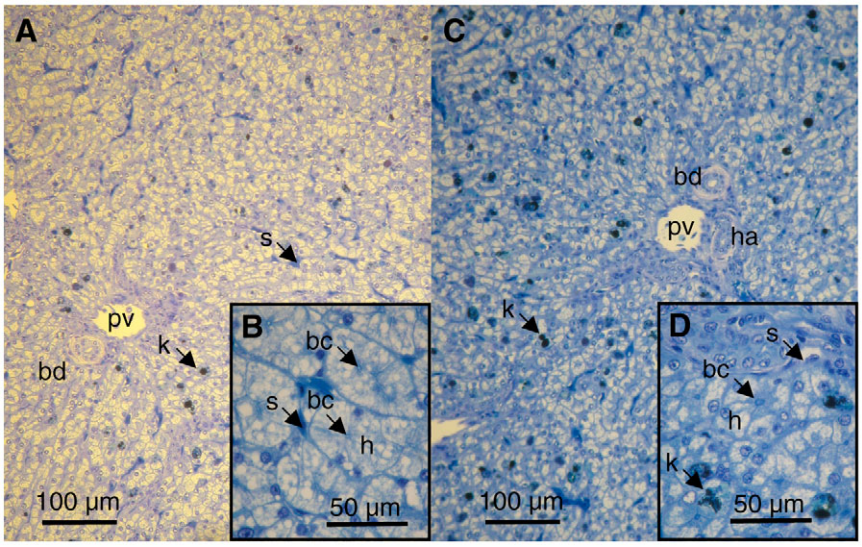


Fig. 8. Light micrographs of the liver of feeding and fasting caimans. (A) Low power micrograph of the liver of a feeding caiman. (B) High power micrograph of the liver tubules of a feeding caiman. (C) Low power micrograph of the liver of a fasting caiman. (D) High power micrograph of the liver tubules of a fasting caiman. bc, bile canaliculus; bd, bile duct; h, hepatocytes; ha, branch of the hepatic artery; k, Kupffer cell; pv, branch of the portal vein; s, sinusoid.

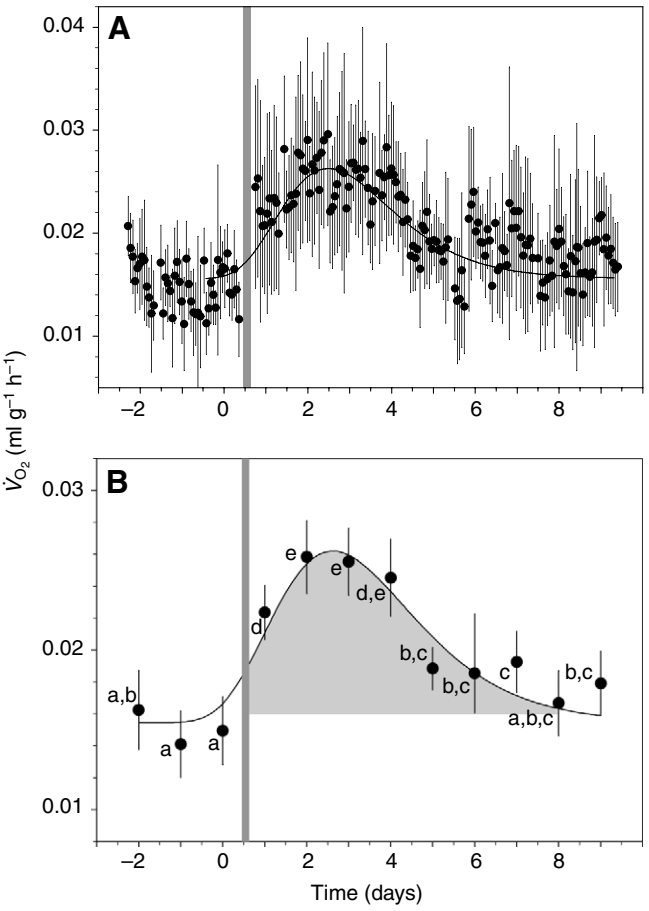


Fig. 9. Oxygen consumption of caimans ($N$=8) for 2 days before feeding and 9 days after feeding. Feeding was around noon of day 0 as indicated by the grey bar. The plotted curves were derived by fitting data to a log normal 4 parameter model. (A) Continuous measurements over the entire experimental period. Values are means of eight individuals; each animal was assessed for 10 min during an 80-min interval. (B) Daily mean $\dot{V}_{O_2}$ derived from data in A. Values are means ± s.d. from all measurement intervals per day for eight individuals. Different letters denote significant difference according to Tukey's HSD *post-hoc* test for comparisons of multiple means; $\alpha$<0.05. The grey shaded area under the curve represents SDA; the vertical bar indicates interruption of the continuous measurements for feeding.

6–9 days after feeding (0.018±0.0026 ml $O_2$ g$^{-1}$ h$^{-1}$). The time resolution of 80 min in Fig. 9 results in some oscillation of the $\dot{V}_{O_2}$ data, obviously related to circadian fluctuations in metabolic rate. To analyze the differences between days, we used RM ANOVA with Tukey's HSD post-hoc test. Within 24 h after feeding $\dot{V}_{O_2}$ had increased significantly as compared to the days before feeding. Peak values at day 2 and day 3 after feeding were significantly different from all other values. Beginning at day 4 after feeding $\dot{V}_{O_2}$ declined, reaching pre-feeding values at day 6–9 after feeding. Results of the post-hoc statistics on daily averages are given in Fig. 9B. SDA was calculated to be 36.1 kJ for an animal with the average body mass of 1.68 kg, or 21.5 kJ kg$^{-1}$.

## Discussion

Broad nosed caimans showed a response to feeding typical for many other ectothermic sauropsids, i.e. a fast and fully reversible increase of the mucosal thickness of the duodenum and the distal small intestine accompanied by a significant increase of oxygen consumption. The range and dynamics of size increase of the gut and increase of metabolic rate were in the same range as described for other sauropsids, i.e. the size changes of the mucosa of the duodenum and the small intestine were in the order of 50–100% within 2–3 days and returned to fasting values within 10 days after feeding. Published data from snakes (Secor and Diamond, 1995; Secor and Diamond, 1997; Jackson and Perry, 2000; Starck and Beese, 2001; Starck and Beese, 2002; Lignot et al., 2005; Starck and Wimmer, 2005) and frogs (Cramp, 2005; Cramp and Franklin, 2005; Cramp et al., 2005) reported the same range of organ size changes.

Published data of SMR in crocodilian species vary because of different experimental temperatures and different body size of the individuals studied. However, mass specific SMR at 30°C of broad nosed caiman was well within the range of published data for *Crocodylus niloticus* (Brown and Loveridge, 1981; Aulie et al., 1989; Aulie and Kanui, 1995), *Alligator mississippiensis* (Coulson et al., 1977; Coulson and Hernandez, 1983; Busk et al., 2000), *Caiman latirostris* (Hernandez and Coulson, 1952) and *Caiman crocodilus* (Bennett and Dawson, 1976).

In broad nosed caimans, oxygen consumption peaked at 0.026 ml $O_2$ g$^{-1}$ h$^{-1}$, i.e. a 1.6-fold increase within 48 h after feeding. A 3–4-fold postprandial increase of metabolic rate was reported for the American alligator (Coulson and Hernandez, 1983; Busk et al., 2000) feeding a meal of 5% and 7.5% of their body mass. A 1.6-fold increase in oxygen consumption has been reported for spectacled caiman (Gatten, 1980), but no information about meal size was provided. The postprandial increase in metabolic rate measured in our study is relatively low compared to that reported in other studies on crocodilians or snakes (Secor, 2005a), but, the extent of SDA depends on temperature, amount of food, food composition, length of the preceding fasting period, age and size (McCue, 2006; Wang et al., 2006), and certainly phylogenetic relationship. It is beyond the scope of this study to test for each of those factors separately. However, the general pattern of postprandial metabolic increase is clearly the same as described for other sauropsids even though it represents the lower margin of the known range (1.6–15-fold increase of metabolic rate). A moderate increase in oxygen consumption, as reported here, is probably related to the relatively small amount of food (7–15% of the animals' body mass). In sit-and-wait foraging snakes that were fed a meal of up to 80% of their own body mass, an 18-fold factorial increase of the metabolic rate has been reported as the extreme (Secor and Diamond, 1995).

Only a few papers have described the normal histology of the gastrointestinal tract (Taguchi, 1920; Kotzé et al., 1992; Kotzé and Soley, 1995; Richardson et al., 2002) and the liver (Storch et al., 1989; Schaffner, 1998; Richardson et al., 2002) of crocodiles. However, none refers to the feeding condition of

the animals, and none gives details about the arrangement of intestinal mucosa epithelial cells, although the figures in the publications are detailed enough to recognize a (pseudo)stratified epithelium, and the fact that a pseudostratified structure of the mucosa epithelium and size changes of the intestines had been mentioned almost 100 years ago (Reese, 1915).

The structural differences described for the mucosa epithelium of the duodenum and the distal small intestine in digesting and fasting caimans are the same as those described for *Python molurus* (Starck and Beese, 2001; Lignot et al., 2005), *Thamnophis sirtalis* (Starck and Beese, 2002), and *Python regius* (Starck and Wimmer, 2005), using LM and TEM. For snakes it had been shown that loading of the enterocytes with lipid droplets and increased blood flow to the small intestine ultimately correlate with a swelling of the villi and the enterocytes (Starck and Beese, 2001; Starck and Beese, 2002; Starck, 2003; Starck et al., 2004; Lignot et al., 2005; Starck, 2005; Starck and Wimmer, 2005). In caimans, the observed structural changes associated with the postprandial response are identical to those observed in snakes. Therefore, we suggest that the size increase of the small intestine is also based on loading of the enterocytes with lipid droplets and, probably, increased blood flow to the mucosa epithelium. Similarly, down-sizing of duodenum and distal small intestine are always associated with ceasing blood flow to the gut and removing of lipid droplets from the enterocytes (to the liver). The identity of all histological, cytological, and ultrastructure details as well as the dynamics of organ size change strongly supports the idea that crocodiles employ the same mechanism for size changes of the gut described in other ectotherm sauropsids. Comparisons can tentatively be extended beyond sauropsids because recent studies (Cramp, 2005; Cramp and Franklin, 2005; Cramp et al., 2005; Starck, 2005) provided detailed descriptions of histological changes associated with feeding and fasting of three frog species. Again, histological and ultrastructure details are the same as described earlier in squamates and here for a crocodile.

Morphometry of size changes of the liver has not provided such unequivocal data as for the small intestine. Whereas we observed highly significant changes in liver fresh mass between the groups of digesting and fasting individuals, the within groups comparisons between days did not render significant differences. Possible explanations are, that the observation time was not long enough to detect significant size changes of the liver, and/or the measurement error by ultrasonography at the chosen image plane is too large to detect short term size changes. A third possible explanation is provided by histology, which showed that the hepatocytes of fasting caimans were still loaded with lipid droplets, thus hepatocytes after 3 months fasting were still full and could not be loaded further. The comparison of fresh mass of liver and between groups, however, showed that size changes occur and are clearly associated with feeding condition. Similar size changes and similar histological changes of the liver have been reported only for snakes (Starck and Beese, 2002; Starck and Wimmer, 2005; Großmann and Starck, 2006). In general, the relative postprandial change in liver size was less than that observed for the small intestine.

Placing this observation in comparative and phylogenetic context with birds and squamates, the caimans show the same features as found in squamates. Birds also adjust gut and liver size to in response to demands of feeding and fasting or in response to diet shifts (Starck, 1996; Dunel-Erb et al., 2001; Starck, 2003; Starck, 2005). However, size changes of the small intestine are based on cell proliferation in the intestinal crypts and cell loss at the tip of the villi. In a phylogenetic context, the most parsimonious conclusion is that the transitional epithelium of caimans and squamates is the plesiomorphic condition. The avian-type flexibility of the gut, based on turn-over of cells, appears to be a derived feature of that clade. Although little is known about the postprandial size changes of the gastrointestinal tract in turtles (Secor and Diamond, 1999) and nothing is known about tuatara (*Sphenodon*) we can expand this comparison beyond sauropsids. Recent data on frogs (Cramp, 2005; Cramp and Franklin, 2005; Cramp et al., 2005) showed that identical changes in the level of cells and tissues occur in digesting and fasting frogs as well as in aestivating frogs (*Cyclorana alboguttata*). Preliminary data from two other anuran species (*Xenopus laevis*, *Ceratophrys cranwellii*) also showed an identical histological pattern associated with postprandial organ size changes of the small intestine (Starck, 2005). We conclude that configuration changes of the intestinal mucosa epithelium based on loading of enterocytes with lipid droplets, and possibly increasing blood flow to the intestines are an ancestral feature of the gut of tetrapods resulting in repeated and reversible organ size changes. Consequently, the same pattern of organ size change of the small intestine and the liver in response to feeding must have been present in their common stem group. We conclude that they must have been perfectly able to tolerate extended fasting periods. Sit-and-wait foraging sauropsids such as giant constrictor snakes and crocodiles employ a phylogenetically ancestral feature to adjust their guts to digesting after long fasting intervals. The ability to change gut size certainly is not a unique adaptation to their specific mode of feeding because it appears in other clades of tetrapods, and without question, it is a functional feature of the gut in adopting to sit-and-wait foraging style. We do not exclude the possibility here that evolution has shaped the postprandial response in sit-and-wait foraging snakes to a wider performance range as compared to other ectothermic sauropsids (Secor, 2001). However, our comparison also does not exclude the option that the described features of the gut emerged as a byproduct of the patterns of lipid absorption and blood perfusion of the gut. Then, organ size changes and the tissue configuration changes may have emerged as an exaptation (Gould and Lewontin, 1979; Gould and Vrba, 1982) and only later became employed in a adaptive context. Within sauropsids, birds have independently evolved a different mechanism of organ size changes that is based on cell proliferation at the base of the villi and cell loss at the tip of

the villi. Similarly, size changes of gut and liver in mammals are also based on cell proliferation and cell loss. Obviously, parallel evolution of homeothermy and more continuous feeding patterns has lead to such convergent pattern of organ size change.

We cordially thank Denis Andrade, Simone Brito, and Joshua Parker for their help during the study in Brazil. Sybille Koch (Jena), Heidi Gensler (Munich) and Cornelius Lemke (Jena) helped with the laboratory work. The study was supported by grant STA 345/8-1 from the German Research Council (DFG) to J.M.S. A.S.A. was supported by CNPq grant.

## References

**Ashworth, C. T. and Lawrence, J. F.** (1966). Electron microscopic study of the role of lipid micelles in intestinal fat absorption. *J. Lipid Res.* **7**, 465-472.

**Aulie, A. and Kanui, T. I.** (1995). Oxygen consumption of eggs and hatchlings of the Nile crocodile (*Crocodylus niloticus*). *Comp. Biochem. Physiol.* **112A**, 99-102.

**Aulie, A., Kanui, T. I. and Maloiy, G. M. O.** (1989). The effects of temperature on oxygen consumption of eggs and hatchlings of the Nile crocodile (*Crocodylus niloticus*). *Comp. Biochem. Physiol.* **93A**, 473-475.

**Bennett, A. F. and Dawson, W. R.** (1976). Metabolism. In *Biology of Reptilia*. Vol. 5 (ed. C. Gans), pp. 127-223. London, New York, San Francisco: Academic Press.

**Böck, P.** (1989). *Romeis' Mikroskopische Technik*. München: Urban and Schwarzenberg.

**Brown, C. R. and Loveridge, J. P.** (1981). The effect of temperature on oxygen consumption and evaporative water loss in *Crocodylus niloticus*. *Comp. Biochem. Physiol.* **69A**, 51-57.

**Busk, M., Overgaard, J., Hicks, J. W., Bennett, A. F. and Wang, T.** (2000). Effects of feeding on arterial blood gases in the American alligator *Alligator mississippiensis*. *J. Exp. Biol.* **203**, 3117-3124.

**Coulson, R. A. and Hernandez, T.** (1983). Alligator metabolism: studies of chemical reactions in vivo. *Comp. Biochem. Physiol.* **74B**, 1-182.

**Coulson, R. A., Hernandez, T. and Herbert, J. D.** (1977). Metabolic rate, enzyme kinetics in vivo. *Comp. Biochem. Physiol.* **56A**, 251-262.

**Cramp, R.** (2005). The effects of aestivation and re-feeding on structure and function of the gut in the green-striped burrowing frog, *Cyclorana alboguttata*. PhD thesis, School of Integrative Biology, University of Queensland, Australia.

**Cramp, R. L. and Franklin, C. E.** (2005). Arousal and re-feeding rapidly restores digestive tract morphology following aestivation in green-striped burrowing frogs. *Comp. Biochem. Physiol.* **142A**, 451-460.

**Cramp, R. L., Franklin, C. E. and Meyer, E. A.** (2005). The impact of prolonged fasting during aestivation on the structure of the small intestine in the green-striped burrowing frog, *Cyclorana alboguttata*. *Acta Zool.* **86**, 13-24.

**Cullum, A. J.** (1997). Comparisons of physiological performance in sexual and asexual whiptail lizards (genus *Cnemidophorus*): implications for the role of heterozygosity. *Am. Nat.* **150**, 24-47.

**Dixon, J. R. and Soini, P.** (1977). The reptiles of upper Amazon basin, Iquitos region, Peru. *Contrib. Biol. Geol.* **12**, 1-91.

**Dunel-Erb, S., Chevalier, C., Laurent, P., Bach, A., Decrock, F. and Le Maho, Y.** (2001). Restoration of the jejunal mucosa in rats refed after prolonged fasting *Comp. Biochem. Physiol.* **129A**, 933-947.

**Ganser, L. R., Hopins, W. A., O'Neil, L., Hasse, S., Roe, J. H. and Sever, D. M.** (2003). Liver histopathology of the southern watersnake, *Nerodia fasciata fasciata*, following chronic exposure to trace element-contaminated prey from a coal ash disposal site. *J. Herpetol.* **37**, 219-226.

**Gatten, R. E.** (1980). Metabolic rates of fasting and recently fed spectacled caimans (*Caiman crocodilus*). *Herpetologica* **36**, 361-364.

**Gorzula, S. J.** (1978). An ecological study of *Caiman crocodilus* inhabiting savanna Lagoons in the Venezuelan Guayana. *Oecologia* **35**, 21-34.

**Gould, S. J. and Lewontin, R. C.** (1979). The spandrels of San Marco and the Panglossian paradigm: a critique of the adaptionist programme. *Proc. R. Soc. Lond. B Biol. Sci.* **205**, 581-598.

**Gould, S. J. and Vrba, E. S.** (1982). Exaptation – a missing term in the science of form. *Paleobiology* **8**, 4-15.

**Green, H. W.** (1997). *The Evolution of Mystery in Nature*. Berkeley: University of Berkeley Press.

**Großmann, J. and Starck, J. M.** (2006). Postprandial responses to feeding in the African rhombig egg-eater (*Dasypeltis scabra*). *Zoology* **109**, 310-317.

**Habold, C., Chevalier, C., Dunel-Erb, S., Foltzer-Jourdainne, C., Le Maho, Y. and Lignot, J.-H.** (2004). Effects of fasting and refeeding on jejunal morphology and cellular activity in rats in relation to depletion of body stores. *Scandinavian J. Gastroenterol.* **39**, 531-539.

**Hernandez, T. and Coulson, R. A.** (1952). Hibernation in the alligator. *Proc. Soc. Exp. Biol. Med.* **79**, 145-149.

**Jackson, K. and Perry, G.** (2000). Changes in intestinal morphology following feeding in the brown treesnake, *Boiga irregularis*. *J. Herpetol.* **34**, 459-462.

**Karasov, W. H., Pinshow, B., Starck, J. M. and Afik, D.** (2004). Alimentary tract changes in fed, food-restricted, fasted and refed migrant blackcaps (*Sylvia atricapilla*). *Physiol. Biochem. Zool.* **77**, 149-160.

**Konarzewski, M. and Starck, J. M.** (2000). Developmental plasticity of the gastrointestinal tract in song thrush nestlings. *Physiol. Biochem. Zool.* **73**, 416-427.

**Kotzé, S. H. and Soley, J. T.** (1995). Scanning electron microscopic study of intestinal mucosa of the nile crocodile (*Crocodylus niloticus*). *J. Morphol.* **225**, 169-178.

**Kotzé, S. H., van der Merwe, N. J., van Aswegen, G. and Smith, G. A.** (1992). A light microscopical study of the intestinal tract of the Nile crocodile (*Crocodylus niloticus,* Laurenti 1768). *Onderstepoort J. Vet. Res.* **59**, 249-252.

**Lignot, J.-H., Helmstetter, C. and Secor, S. M.** (2005). Postprandial morphological response of the intestinal epithelium of the Burmese python (*Python molurus*). *Comp. Biochem. Physiol.* **141A**, 280-291.

**McCue, M. D.** (2006). Specific dynamic action: a century of investigation. *Comp. Biochem. Physiol.* **144A**, 381-394.

**McCue, M. D.** (2007). Snakes survive prolonged fasting by employing supply-side and demand-side economic strategies. *Zoology* **110** In press.

**Overgaard, J., Andersen, J. B. and Wang, T.** (2002). The effects of fasting duration on the metabolic response in Python: an evaluation of the energetic costs associated with gastrointestinal growth and up-regulation. *Physiol. Biochem. Zool.* **75**, 360-368.

**Peterson, C. C.** (1990). Paradoxically low metabolic rate of the diurnal gecko *Rhoptropus afer*. *Copeia* **1990**, 233-237.

**Pope, C. H.** (1961). *The Giant Snakes*. New York: A. A. Knopf.

**Reese, A. M.** (1915). *The Alligator and its Allies*. New York, London: G. P. Putnam's Sons.

**Richardson, K. C., Webb, G. J. W. and Manolis, S. C.** (2002). *Crocodiles: Inside Out. A Guide to the Crocodilians and their Functional Morphology*. Chipping Norton, Australia: Surrey Beatty & Sons.

**Schaffner, F.** (1998). The liver. In *Biology of Reptilia*. Vol. 19 (ed. C. Gans and A. S. Gaunt), pp. 297-374. Ithaca, NY: SSAR Press.

**Schaller, G. B. and Crawshaw, J. P. G.** (1982). Fishing behavior of Paraguayan caiman (*Caiman crocodilus*). *Copeia* **1982**, 66-72.

**Scott, N. J., Jr, Aquino, A. L. and Lee, A. F.** (1990). Distribution, habitats and conservation of the caimans (Alligatoridae) of Paraguay. *Vida Silvestre Neotropical* **2**, 43-51.

**Secor, S. M.** (2001). Regulation of digestive performance: a proposed adaptive response. *Comp. Biochem. Physiol.* **128A**, 565-577.

**Secor, S. M.** (2005a). Evolutionary and cellular mechanisms regulating intestinal performance of amphibians and reptiles. *Integr. Comp. Biol.* **45**, 282-294.

**Secor, S. M.** (2005b). Physiological responses to feeding, fasting and estivation for anurans. *J. Exp. Biol.* **208**, 2595-2608.

**Secor, S. M. and Diamond, J.** (1995). Adaptive responses to feeding in Burmese pythons: pay before pumping. *J. Exp. Biol.* **198**, 1313-1325.

**Secor, S. M. and Diamond, J.** (1997). Determinants of the postfeeding metabolic response of Burmese pythons (*Python molurus*). *Physiol. Biochem. Zool.* **70**, 202-212.

**Secor, S. M. and Diamond, J.** (1998). A vertebrate model of extreme physiological regulation. *Nature* **395**, 659-662.

**Secor, S. M. and Diamond, J.** (1999). Maintenance of digestive performance in the turtles *Chelydra serpentina*, *Sternotherus odoratus*, and *Trachemys script*. *Copeia* **1999**, 75-84.

**Secor, S. M. and Diamond, J.** (2000). Evolution of regulatory responses to feeding in snakes. *Physiol. Biochem. Zool.* **73**, 123-141.

**Secor, S. M., Stein, E. D. and Diamond, J.** (1994). Rapid upregulation of

snake intestine in response to feeding: a new model of intestinal adaptation. *Am. J. Physiol.* **266**, G695-G705.

**Starck, J. M.** (1996). Phenotypic plasticity, cellular dynamics, and epithelial turnover of the intestine of Japanese quail (*Coturnix coturnix japonica*). *J. Zool. Lond.* **238**, 53-79.

**Starck, J. M.** (2003). Shaping up: how vertebrates adjusts their morphology to changing environmental conditions. *Anim. Biol.* **53**, 245-257.

**Starck, J. M.** (2005). Structural flexibility of the digestive system of tetrapods. Patterns and processes on the level of cells and tissues. In *Physiological and Ecological Adaptations to Feeding in Vertebrates* (ed. J. M. Starck and T. Wang), pp. 175-200. Enfield, NH: Science Publishers.

**Starck, J. M. and Beese, K.** (2001). Structural flexibility of the intestine of Burmese python in response to feeding. *J. Exp. Biol.* **204**, 325-335.

**Starck, J. M. and Beese, K.** (2002). Structural flexibility of the small intestine and liver of garter snakes in response to feeding and fasting. *J. Exp. Biol.* **205**, 1377-1388.

**Starck, J. M. and Wimmer, C.** (2005). Patterns of blood flow during the postprandial response in ball pythons, *Python regius*. *J. Exp. Biol.* **208**, 881-889.

**Starck, J. M., Moser, P., Werner, R. A. and Linke, P.** (2004). Pythons metabolize prey to fuel the response to feeding. *Proc. R. Soc. Lond. B Biol. Sci.* **271**, 903-908.

**Storch, V., Braunbeck, T. and Waitkuwait, W. E.** (1989). The liver of the West African crocodile *Osteolaemus tetraspis*. An ultrastructural study. *J. Submicrosc. Cytol. Pathol.* **21**, 317-327.

**Taguchi, H.** (1920). Beiträge zur Kenntnis über die feinere Struktur der Eingeweideorgane der Krokodile. *Mittl. Med. Fakult. Kaiserl. Univ. Tokyo* **25**, 119-188.

**Vleck, D.** (1987). Measurement of $O_2$ consumption, $CO_2$ production, and water vapor production in a closed system. *J. Appl. Physiol.* **62**, 2103-2106.

**Wang, T., Hung, C. C. Y. and Randall, D. J.** (2006). The comparative physiology of food deprivation: from feast to famine. *Annu. Rev. Physiol.* **68**, 223-251.